J Polym Res (2017) 24: 227
https://doi.org/10.1007/s10965-017-1382-5

ORIGINAL PAPER

Preparation and enhanced mechanical properties of hydroxyapatite hybrid hydrogels via novel photocatalytic polymerization

Da-Jhan Chiu[1] · Ying Li[2] · Chi-Kuang Feng[3] · Mu-Rong Yang[1] · Ko-Shao Chen[1,2] · Wojciech Swieszkowski[4]

Received: 29 July 2017 / Accepted: 1 November 2017 / Published online: 21 November 2017

Abstract Hydroxyapatite (HA) hybridized poly(N-isopropylacrylamide)-co-acrylic acid (PNIPAM-co-AAc) hydrogel on thermoplastic polyurethane (TPU) were successfully prepared via photocatalytic polymerization technique. Low temperature plasma processing of HMDSZ and O_2 plasma were deposition on substrate. The HA/hydrogel were stabilized by HA of which the wettability was modified by calcium nitrate and ammonium phosphate dibasic. The HA gradually increases with the increase of time cycles. The deposition of organic silicone group by the HMDSZ on the TPU substrate is hydrophobic surface. When deposition of O_2, the water contact angles (WCA) was changed to <10° and surface hydrophilicity. The materials were characterized by OM, SEM, FT-IR, XPS and XRD. The results showed that the NIPAM: AAc (1:1 mol) polymers possess macropores ranging from 2 to 20 μm, and their large numbers of carboxyl groups and hydroxyl groups result in a favorable adsorption capacity for HA. Swelling studies indicated that NIPAM: AAc (1:1 mol) was 446 ± 0.3%. This work provided a promising alternative method for the fabrication of polymer materials with tunable and interconnected pores structures for the HA.

Keywords Low temperature plasma · Photocatalytic polymerization · Composite hydrogel · Hydroxyapatite

Mu-Rong Yang is a co-advisor for Da-Jhan Chiu at Tatung University

Electronic supplementary material The online version of this article (https://doi.org/10.1007/s10965-017-1382-5) contains supplementary material, which is available to authorized users.

✉ Ko-Shao Chen
cksttu@gmail.com

[1] Department of Materials Engineering, Tatung University, Taipei, Taiwan

[2] Center for Thin Film Technologies and Applications (CTFTA), Ming Chi University of Technology, Taipei, Taiwan

[3] Department of Orthopaedics and Traumatology, Veterans General Hospital-Taipei, Taipei, Taiwan

[4] Faculty of Materials Science and Engineering, Warsaw University of Technology, Warsaw, Poland

Introduction

Polymers with "smart" behaviour are in the focus of a variety of research fields. This category of substances is classified as "smart or intelligent materials" because these hydrogel can undergo conformation changes in response to alterations in environmental conditions. Hydrogel are physically or chemically cross-linked particles with a network structure that is swollen in a suitable solvent. Hydrogels can swell and retain a large amount of water or biological fluid within the structure without dissolving. In the preparation of polymeric hydrogel, there are in principle four methods that have been reported, namely emulsion polymerization [1], anionic copolymerization [2], chemical cross-linking of neighboring chains [3], radical polymerization [4, 5] and microemulsion polymerization [6].

The most studied class of responsive polymers are temperature sensitive poly(acrylamide), specifically poly(N-isopropylacrylamide) (PNIPAM). PNIPAM, a typical temperature sensitive hydrogel, can be fabricated as an interpenetrating/semi-interpenetrating polymer network (IPN/SIPN) or a copolymer, depending on the doping substances and methods. One reason is their high impact for applications. Besides, the collapse transition of PNIPAM-based hydrogel is also a key problem that is involved in many applications such as biomedicine and catalysis, which is determined mainly by the thermal collapse behavior. Chemically cross-linked PNIPAM hydrogel and PNIPAM with different

amounts of acrylic acid (AAc) groups (PNIPAM-co-PAA) were synthesized and the temperature-induced aggregation behaviors of aqueous suspensions of these hydrogel were investigated mainly with the aid of dynamic light scattering (DLS) and turbidimetry [7]. Thermosensitive coatings are fabricated by spin-coating of hydrogel consisting of the crosslinked copolymer PNIPAM-co-AAc on silicon wafers [8]. The collapse of PNIPAM-co-AAc hydrogel suspensions is studied by dielectric spectroscopy in a frequency range from 40 Hz to 110 MHz as a function of temperature [9]. It describes the photoluminescence (PL) response of PNIPAM-based core/shell hydrogel nanoparticles with dual emission, which is obtained by emulsion polymerization with potassium persulfate, consisting of the thermo- and pH-responsive copolymers of PNIPAM and AAc [10]. For the hydrogel with semi-interpenetrating network structure, although interpenetration can be realized by controlling the preparation process, the two networks are actually phase-separated from the hydrogel view: linear PAAc forms a domain in the PNIPAM network. For the PNIPAM-co-AAc hydrogel, the monomers AAc are randomly bonded to the network [11–13]. A convenient approach has been developed for the preparation of microsize hydrogels composed of crosslinked AAc and PNIPAM. This indicates that PNIPAM-co-AAc hydrogel might be a potential drug delivery carriers especially for water-soluble or polypeptide drugs [14].

Hydroxyapatite (HA) is the principal inorganic constituent of bone and tooth in vertebrates, thus, HA materials have excellent biocompatibility, high thermal stability and promising applications in various biomedical fields [15, 16]. HA is widespread in human body in the form of solid or ionic state, and is dynamically involved in bone resorption and reconstruction and metabolic processes of calcium and phosphorus ions. Several synthetic methods have been reported for HA, including the solvothermal/hydrothermal method [17–21], microwave-assisted synthesis [22, 23], hard template using porous anodic aluminum oxide [24], sol-gel process [25], and reverse micelles [26]. So most of commercial bone replacement materials, such as ceramic HA, coralline HA and nylon-66(PA66)/HA composites, contain a certain amount of HA.

Furthermore, due to their water-soluble and biocompatible properties, intelligent polymers (PNIPAM and AAc) might be ideal materials to bridge the gap between biological machines and multi-functional actuators. Photocatalytic processes create radicals in the system and play an important role in the photocatalytic reaction. Therefore, these radicals might be a promising candidate as a photo-initiator for utilization in radical polymerization processes. In this work, we utilized the radical for the photoinitiation of the fabrication of the hydrogel composite. The common methods for the synthesis of HA are the immersed method. HA/hydrogels have been used in many fields, such as tissue engineering, drug delivery and divalent heavy metal ion removal. However, it is still a big challenge to devise an efficient approach for fabricating multi-sensitive smart solid/polymer/liquid interfaces, which is an important step towards the utilization of surface-confined smart polymers as building blocks for biomimetics.

Materials and methods

Materials

Thermoplastic polyurethane (TPU) was cut in 1 × 1 cm^2 in area as a substrate. Hexamethyldisilazan ($[CH_3)_3Si]_2NH$, HMDSZ), N-isopropylacrylamide (NIPAM) and riboflavin (($C_{17}H_{20}N_4O_6$), Vitamin B_2) were purchased from Ferak Chemicals Ltd.. Acrylic acid ($C_3H_4O_2$, AAc), ammonium persulfate ($(NH_4)_2S_2O_8$), APS), N, N-methylene-bis-acrylamide, NMBA), calcium nitrate ($Ca(NO_3)_2$) and ammonium phosphate dibasic $(NH_4)_2HPO_4$ were purchased from Sigma Aldrich Chemical Co. (St. Louis, MO). The reagents used were of analytical grade or of the highest purity that was available commercially, and they were used as received. All solutions were prepared with deionized water at a resistivity not less than 18 M Ω cm (Milli-Q, Bedford, MA).

Low temperature plasma processing

The TPU were first cleaned ultrasonically with cleaning agent and distilled water for 15 min, followed by further cleaning with ethyl alcohol ultrasonically for 15 min, and then dried at room temperature. Plasma at frequency of 13.56 MHz radio frequency (RF) generators (model PD-2S manufactured by SAMCO Co.) for deposition was used in this study. A vacuum pump was employed to provide a low-pressure environment. The bell-jar reaction chamber was evacuated to less than 30 mTorr before plasma deposition treatment. When the pressure became stable, HMDSZ monomer were introduced into the reaction chamber and maintained at a constant pressure by adjusting the micro-throttle valve in the reactor-inlet tube. After pressure became stable, the plasma glow discharge treatment was started. The substrate was keep at room temperature during the treatment, which was performed under the following conditions, input power and the treatment time is 5 min, and the amount of monomers 100 mTorr, respectively. After HMDSZ plasma deposition on substrate and followed by oxygen plasma treatment. Figure 1a shows the schematic of HMDSZ or O_2 plasma equipment.

Synthesis of composite hydrogel

The plasma-treated TPU substrate was further modified by placing it in NIPAM or AAc solution for grafting polymerization. In a typical polymerization of NIPAM, 21.2 mg of APS,

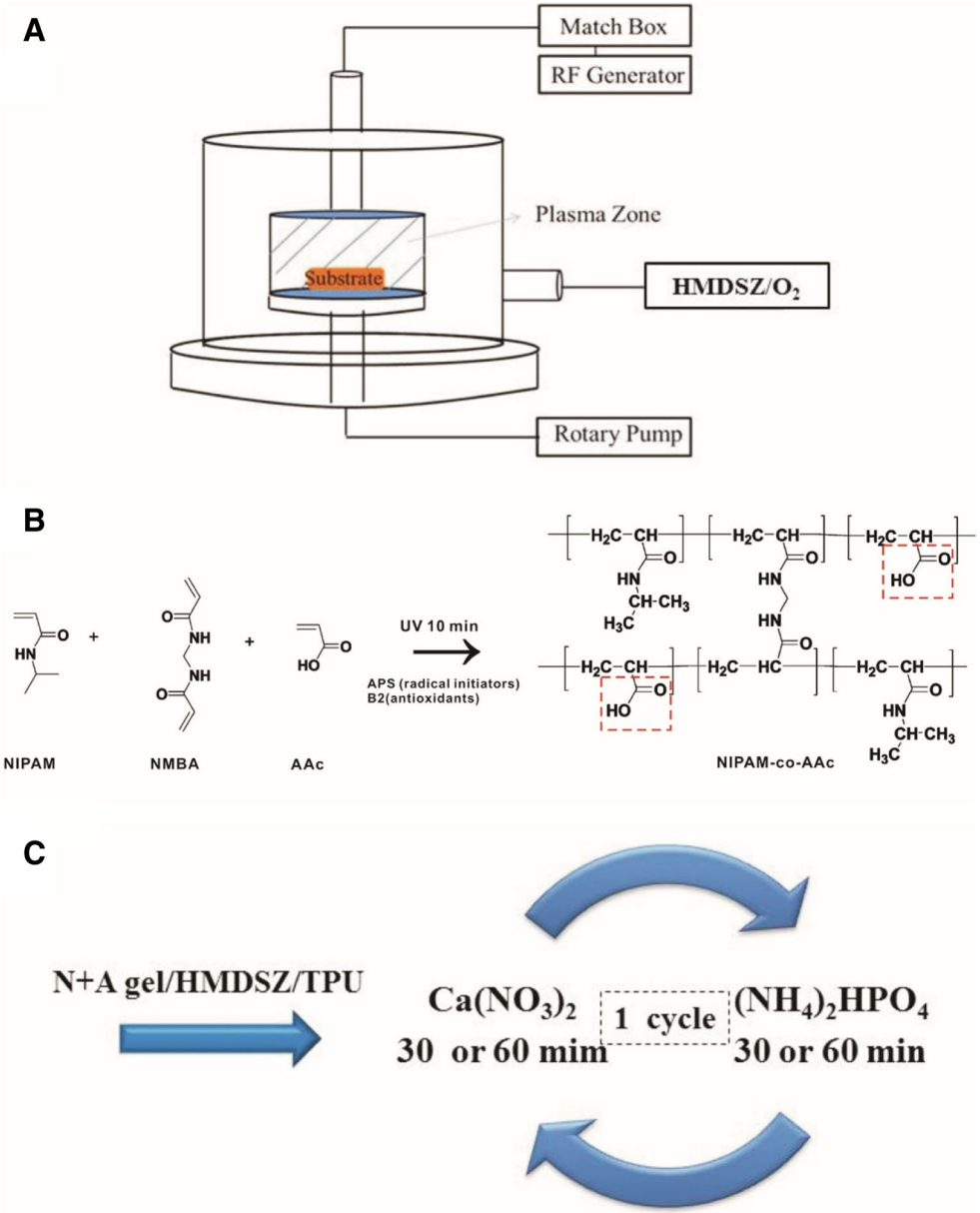

Fig. 1 Schematic diagram of (**a**) the HMDSZ/O_2 plasma deposition on substrate (**b**) NIPAM- co-AAc reaction and (**c**) the TPU were soaked for immobilized hydroxyapatite (HA)

37.0 mg of NMBA, and B_2 as antioxidants were dissolved in aqueous solution (20 ml) containing 0.263 g of NIPAM. Remove the air (O_2) by blowing with N_2 over the surface of the material. After the UV light-induced graft polymerization with NIPAM hydrogels, the specimen was soaked in solution 10 min as show in Fig. 1b NIPAM-co-AAc reaction. In Table 1 shows dependence of the amount of monomers ration of PNIPAM-co-AAc. After grafting step, the TPU were soaked in solutions containing 0.3 M $Ca(NO_3)_2$ and 0.18 M $(NH_4)_2HPO_4$ for immobilized hydroxyapatite (HA). The one cycle of first immobilized in 0.3 M $Ca(NO_3)$ then transfer to $(NH_4)_2HPO_4$. We repeat 3 cycles and each cycle soaking 1 h or 2 h on shaker at 50 rpm for control the morphology of HA on polymer process. The unreacted substance was removed by washing with deionized water. The flow chart of experiments is shown in Fig. 1c.

Table 1 Feed compositions of NIPAAm-co-AAc composite hydrogels

	NIPAAm (mM)	AAc (mM)	DI water (mL)
NIPAAm	11.66	–	19.41
AAc	–	11.66	19.62
N3A1	8.74	2.91	19.8
N1A1	5.83	5.83	19.24
N1A3	2.91	8.74	20

APS: 21.2 mg, NMBA: 37.0 mg, B_2: 5 mL

Swelling studies

The swelling kinetics of the gels was measured at 25 °C. After water was wiped from the surface by using filter paper, the swelling ratio (SRs) of the hydrogels were recorded during swelling at regular intervals (Eq. (1)). Where W_s is the weight of the swelling gel at different time points, and W_d is the weight of the dry gel.

$$SR = (W_s - W_d)/W_d \times 100\% \quad (1)$$

Characterization of surface

The water contact angles (WCA) on the surfaces of HMDSZ and O_2 deposited samples as well as on the surfaces were measured by the sessile drop method with distilled water. The water drops were observed at room temperature by a CCD camera made by AnMo Electronics. Each WCA value appearing in this report was the average of three measurements. Lower water contact angle implies hydrophilicity. The macrostructure and macroscopic phenomenon of the hydrogel on the TPU were obtained by optical microscope (OM, Olympus BHM and Nikon SMZ-2 T). Morphological images taken on the treated samples were obtained with a HITCHI S-3400 N scanning electron microscope (SEM) operating at acceleration voltage of 10 kV. The samples were coated with a platinum layer before placing in the chamber to prevent charging.

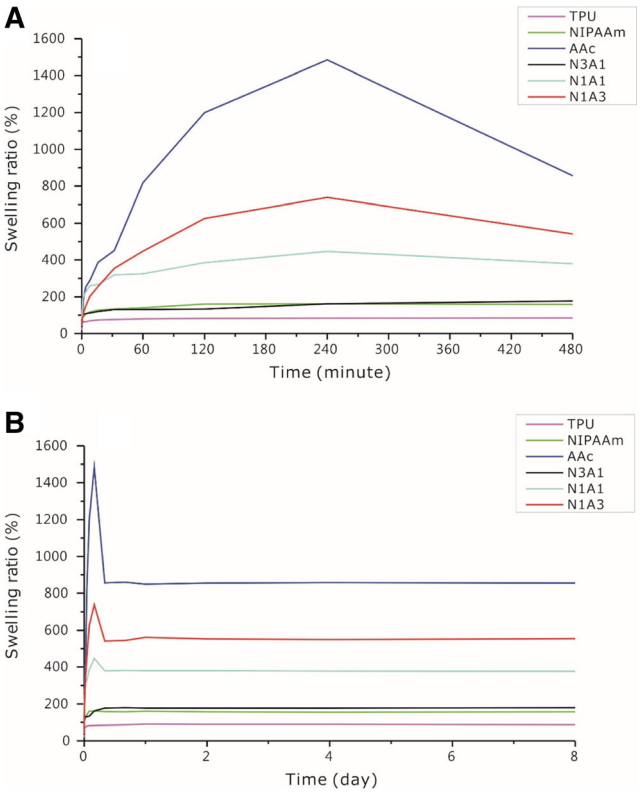

Fig. 2 NIPAM: AAc different ratio effects swelling ratio of the hydrogel at (**a**) 480 min and (**b**) 8 days

Characterization methods

Fourier transformation infrared (FT-IR) spectra were measured by Jasco 6200-type spectrometer. The sample suspension was lyophilized to dry powder, and the obtained dried powder was mixed with KBr and pressed to a plate for measurement. X-ray diffraction (XRD) was used to identify the HA on the hydrogel. The XRD analyses were performed using the PANalytical-X'Pert PRO MPD (Cu radiation, $\lambda = 0.1546$ nm) operating at 40 kV and 40 mA. The X-ray photoelectron spectroscopy (XPS) analysis was performed using the VG ESCA Scientific Theta Probe instrument excited by Al Kα (1486.6 eV) X-ray to produce photoelectrons at a base pressure of 5×10^{-10} mbar in the analysis chamber. The XPS peaks were deconvoluted to determine the precise locations and areas, and the full width half value of each deconvoluted peak was set to be the same.

Results and discussion

Properties of hydrogels

The equilibrium fold swelling of hydrogel composites is shown in Fig. 2. Swelling studies indicated that equilibrium swelling of the hydrogel composites had been reached after being immersed in PBS different time (Fig. 2a). Swelling

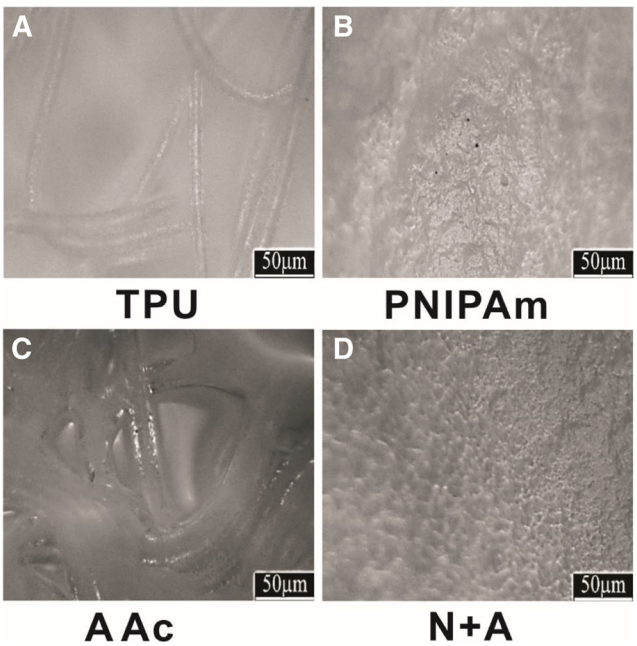

Fig. 3 The macrostructure of hydrogel on the TPU were obtained by optical microscope. **a** TPU (**b**) NIPAM, (**c**) AAc and (**d**) NIPAM-co-AAc hydrogel

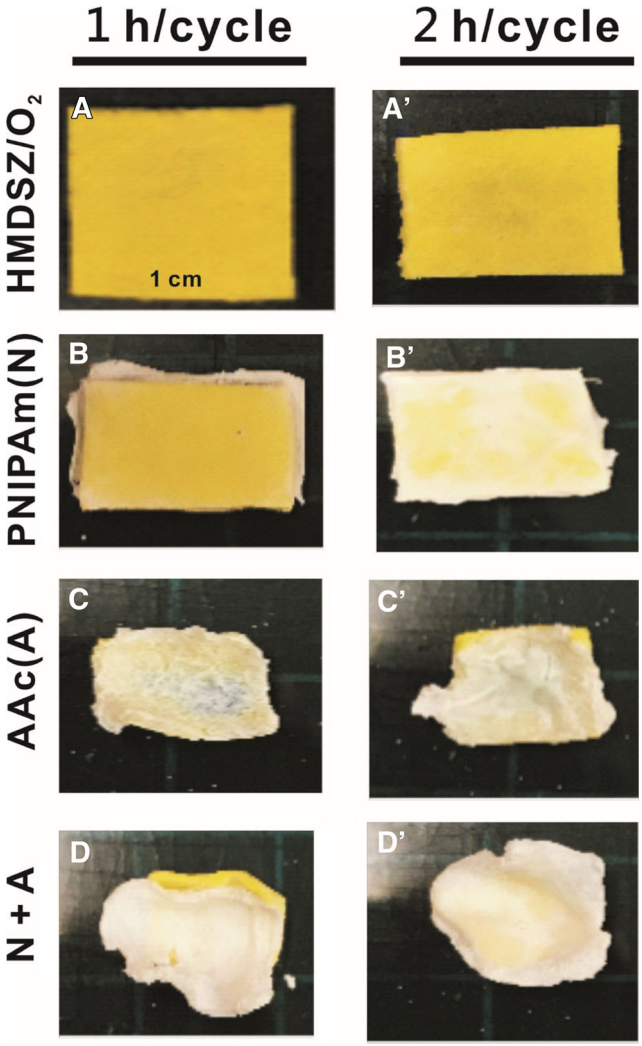

Fig. 4 Digital photos of (**a**) HDMSZ/O_2 (**b**) NIPAM, (**c**) AAc and (**d**) NIPAM -co-AAc hydrogel immobilized of hydroxyapatite (HA) in 1 or 2 h/cycle

ratios of the hydrogels remained the same afterwards for the 8 day culture period (Fig. 2b). At 4 h, the AAc hydrogel had a swelling ratio of 1485 ± 0.3%, which was statistically higher than that of all the other hydrogel formulations. In addition, AAc hydrogel composites had a statistically higher swelling ratio than either NIPAM: AAc (1:3 mol) (738 ± 0.4%) or NIPAM: AAc (1:1 mol) (446 ± 0.3%). Swelling ratios was 100% and no statistical difference between NIPAM and NIPAM: AAc (3:1 mol). The results indicated that swelling ratio increased as the AAc molecular weight in the swelling ratios formulation increased. Sol fraction of hydrogel composites over time is shown in Fig. 2b. For each hydrogel formulation, there was little change in sol fraction over time after 8 h. However, TPU had a significantly lower sol fraction than AAc, NIPAM, NIPAM: AAc (3:1 mol), NIPAM: AAc (1:1 mol) and NIPAM: AAc (1:3 mol) at each time point.

Table 3 Prepared with different amount (mg/cm^2) and weight ratios (%) of monomer hydrogel

	NIPAM	AAc	N3A1	N1A1	N1A3
Amount (mg/cm^2)	10.8	21.8	15.0	16.0	13.4
Weight ratios (%)	49.1	102.8	66.1	78.5	61.4

Morphology of composite hydrogel/HA

Since the synthesized hydrogel were negatively charged it was necessary to use a positively charged substrate. This can be achieved using the deposition of branched SiO_x on a TPU substrate. The TPU layer also leads to an increase of the surface roughness and allows for the formation of entanglements with the dangling ends on the hydrogel surface. The macrostructure and macroscopic phenomenon of the hydrogel on the TPU were obtained by optical microscope (OM) in Fig. 3. One type of NIPAM hydrogel consist of only crosslinked NIPAM chains without incorporated acid group. Pure PNIPAM hydrogel demonstrate a sharp transition at the temperature of about 30–31 °C. The PNIPAM copolymer with mainly COOH containing comonomers were already synthesized. The other hydrogel types (AAc and NIPAM-co-AAc) have both of charged acid groups. In these studies copolymer hydrogel containing chargeable groups were used to increase the adsorption by means of electrostatic interaction. This means that all carboxyl groups of the AAc monomer are protonated have some surface charges introduced by the initiator during the synthesis. With increasing AAc content, the second transition step becomes more pronounced as already described. Hydrogel with the highest AAc content exhibit two very well separated and resolved transition steps.

The simultaneous cross-linking of hydrogel and immobilized of hydroxyapatite (HA) showed great influence on the structure and properties, and even the appearance of

Table 2 Prepared with different amount of monomer hydrogel and comparison[a] with different time per cycle for HA (mg/cm^2) and weight ratios (%)[b]

	NIPAAm	AAc	N3A1	N1A1	N1A3
1 h/cycle	4.5 (113%)	38.6(965%)	34.5(863%)	47.5(1188%)	40.2(1005%)
2 h/cycle	14 (326%)	48.8(1134%)	44.2(1028%)	57.6(1340%)	50.4(1172%)

[a] The TPU/HMDSZ/O_2 per 1 h and 2 h cycle for HA were 4.0 and 4.3 (mg/cm^2)

[b] Weight ratios (%): (W_{sample}/ $W_{TPU/HMDSZ/O2}$) × 100%

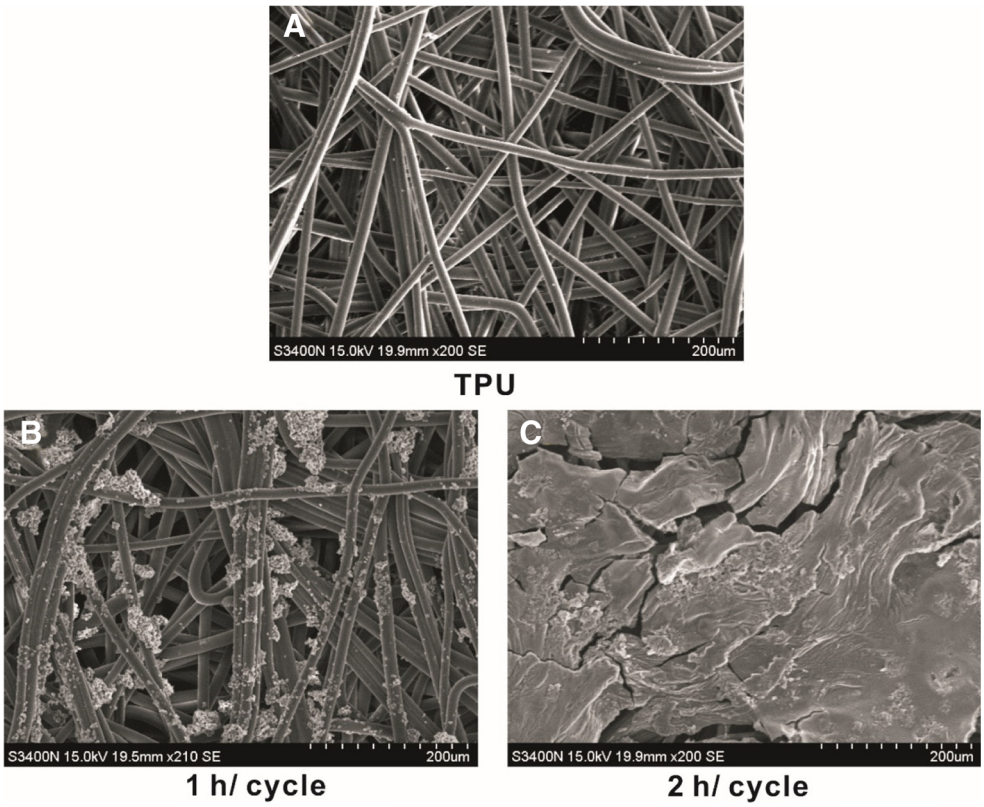

Fig. 5 SEM imaging of (**a**) TPU, NIPAM-co-AAc hydrogel with HA (**b**) 1 h/cycle and (**c**) 2 h/cycle

the UV light-induced graft polymerization hydrogels. Digital photos of three hydrogels prepared with different amount of monomer, namely, HMDSZ/O_2, NIPAM, AAc and NIPAM-co-AAc were shown in Fig. 4 in comparison with different time per cycle. The Table 2 show prepared with different amount of monomer hydrogel and comparison with different time per cycle for HA (mg/cm^2) and weight ratios (%). The Table 3 prepared with different amount (mg/cm^2) and weight ratios (%) of monomer hydrogel. The results showed that the NIPAM: AAc (1:1 mol) polymers have large numbers of carboxyl groups and hydroxyl groups result in a favorable adsorption capacity for HA. The SEM micrographs for different regions of bilayered gradient PNIPAM-co-AAc/HA composite hydrogels prepared by different time cycles were shown in Fig. 5. The HA gradually increases with the increase of time cycles. In Fig. 5b, particles with the size of 2–20 μm uniformly distribute with in the TPU substrates. As it was expected, the hydrodynamic radius increases with increasing AAc content because of the increasing electrostatic repulsion between the polymer chains and an increase in the osmotic pressure. The structure of HA can be observed both on 1 h and 2 h per cycle. Alternate soaking process 2 h per cycle were more HA immobilized than 1 h per cycle. The pK_a of PNIPAM-co-AAc chains is about 5.5. The ionization degree of PNIPAM-co-AAc increases with pH. At a pH value below the pK_a of the PNIPAM-co-AAc chains, most carboxylic acid groups are protonated and the surface of the HA is almost uncharged.

Surface of composite hydrogel/HA

In Fig. 6, the WCA of the TPU surface prior to plasma deposition and hydrogel were measured. The WCA of TPU was 120.0 ± 4.4°. Low temperature plasma of HMDSZ and O_2 deposition obtained from 130.4 ± 4.5° to <10°. The deposition of organic silicone group by the HMDSZ on the TPU substrate is hydrophobic surface. When deposition of O_2, the WCA was changed to <10° and surface hydrophilicity. The NIPAM and AAc hydrogel on TPU of WCA were 114.1 ± 4.5° and <10°. The structure of AAc contain -COOH hydrophilic functional group. The simultaneous cross-linking of NIPAM and AAc hydrogel of WAC was 75.5 ± 4.3°. As mole ratio of AAc increase, surface shown more hydrophilic.

Characterization of composite hydrogel/HA

FT-IR spectra of hydrogel/HA was shown in Fig. 7. The PNIPAM-co-AAc networks, FT-IR spectrum exhibits the characteristic absorption bands of PNIPAM 1664 cm^{-1} for C = O and AAc 3082 cm^{-1} for N-H. The pure SA hydrogel, the stretching mode of C = O and bending or stretching mode of -COOH of sodium alginate correspond to the absorption bands at about 1614, 1417 cm^{-1} [27]. Compare with different time per cycle, the HA characteristic peak show at 560, 606 cm^{-1} for P-O and 3600–3100 cm^{-1} presenting a wide characteristic band for water molecules adsorbed on the surface of powder. The

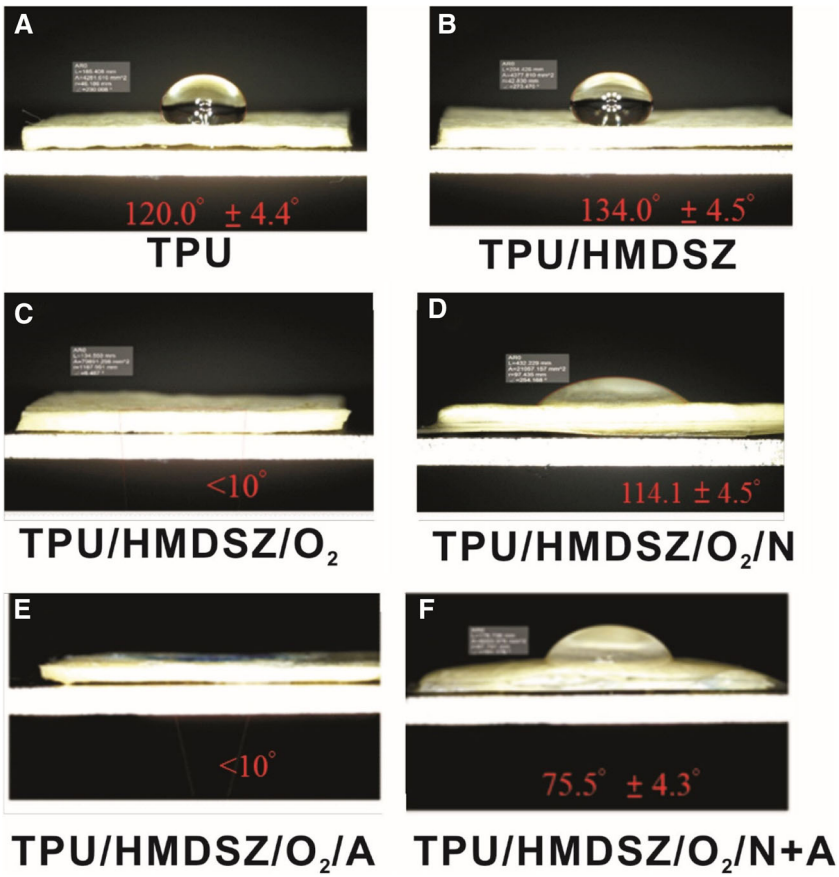

Fig. 6 The WCA imaging of (**a**) TPU, (**b**) HDMSZ, (**c**) HDMSZ/O_2, (**d**) NIPAM, (**e**) AAc, (**f**) NIPAM-co-AAc hydrogel

FTIR spectrum of the HANWs exhibits absorption peaks at around 1097 and 1028 cm^{-1}, which originate from the asymmetric and symmetric stretching modes ofthe PO_4^{3-} group. The absorption peaks at around 634, 603 and 561 $cm^{-1}$are assigned to the bending mode of the O-P-O bond of the PO_4^{3-} group [27]. In addition, the characteristic band corresponding to the carbonyl group in AAc is also absent, resulting from ionization of AAc after alkalization treatment. For PNIPAM the intermolecular interaction includes: hydrogen bonding interaction of NIPAM–H_2O and the hydrophobic interaction of PNIPAM dependent isopropyl groups as well as that of the backbone.

Figure 8 shows the XRD pattern of the HA treated different time in the hydrogel networks. The peaks of the HA at 25.35°and 31.23°were assigned to reflections on the (002) and (211) planes of the face-centered cubic HA, respectively, confirming that HA existed in the hydrogel. Typical two peaks at around 26 and 32° were observed and were assigned as the main peaks for the HAp crystals [28].

XPS wide scan (Fig. 9) identified carbon, nitrogen, oxygen, calcium, and phosphor as the major constituents of HA, as expected. We can confirm the strong development of C1s, N1 s, O1s and Ca2p lines for HA, respectively. The intensity of an O 1 s shake-up satellite correlates with the phosphate oxygen content. The intensity of P2p3 and N1 s signals for HA is relatively weak. On the other hand, O 1 s and Ca2p3 for HA show strong signals. Together with the Ca/P and O/Ca XPS peak ratios, this feature helps provide identification of the CaP phase(s) present in the surface of unknown samples and establish their mole fractions, as proven with a bone sample. PNIPAM-co-AAc/HA the atomic (%) of C1s (14.85%) and

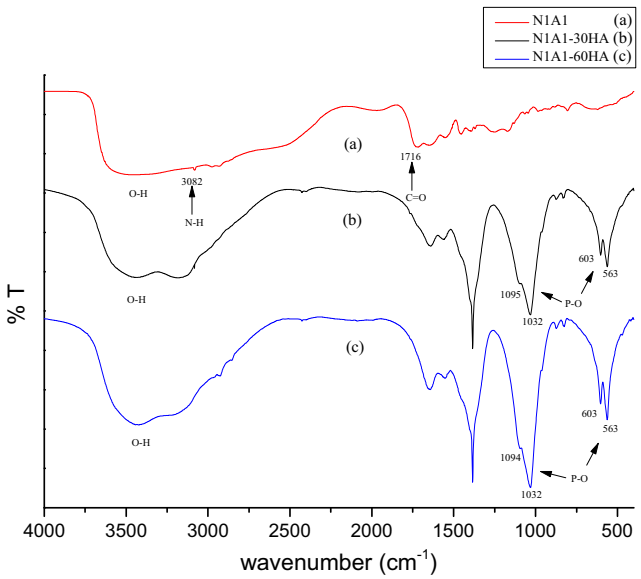

Fig. 7 FTIR spectra of HA with different cycle time

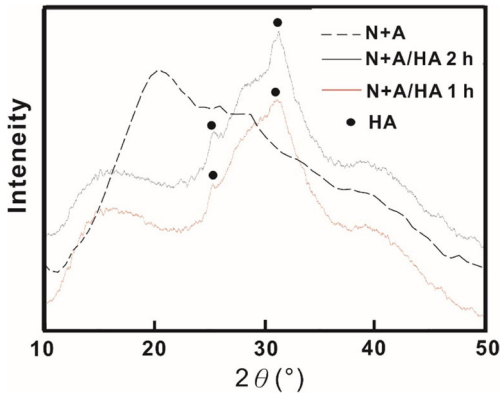

Fig. 8 XRD patterns: the patterns are shifted vertically for better clarity. Characteristic HA diffraction maxima are depicted as (•)

N1 s (1.36%) was decreased, but the O1s (48.09%) and Ca2p (18%) was increased than PNIPAM /HA group. Contributions from carbonate impurities can be quantified using its C 1 s peak at 283.4 eV and subtracted from the O 1 s line shape to aid identification.

Conclusions

Chemically cross-linked poly(N-isopropylacrylamide) (PNIPAM) hydrogels and PNIPAM with different amounts of acrylic acid groups (PNIPAM-co-PAA) were synthesized. The WCA of TPU was 120.0 ± 4.4°. Low temperature plasma of HMDSZ and O_2 deposition obtained from 130.4 ± 4.5° to <10°. The deposition of organic silicone group by the HMDSZ on the TPU substrate is hydrophobic surface. When deposition of O_2, the WCA was changed to <10° and surface hydrophilicity. The NIPAM and AAc hydrogel on TPU of WCA were 114.1 ± 4.5° and <10°. The structure of AAc contain -COOH hydrophilic functional group. The simultaneous cross-linking of NIPAM and AAc hydrogel of WAC was 75.5 ± 4.3°. As mole ratio of AAc increase, surface shown more hydrophilic. Swelling ratios of the hydrogels remained the same afterwards for the 8 day culture period. The AAc hydrogel had a swelling ratio of 1485 ± 0.3%, which was statistically higher than that of all the other hydrogel formulations. In addition, AAc hydrogel composites had a statistically higher swelling ratio than either NIPAM: AAc (1:3 mol) (738 ± 0.4%) or NIPAM: AAc (1:1 mol) (446 ± 0.3%). The results indicated that swelling ratio increased as the AAC molecular weight in the swelling ratios formulation increased.

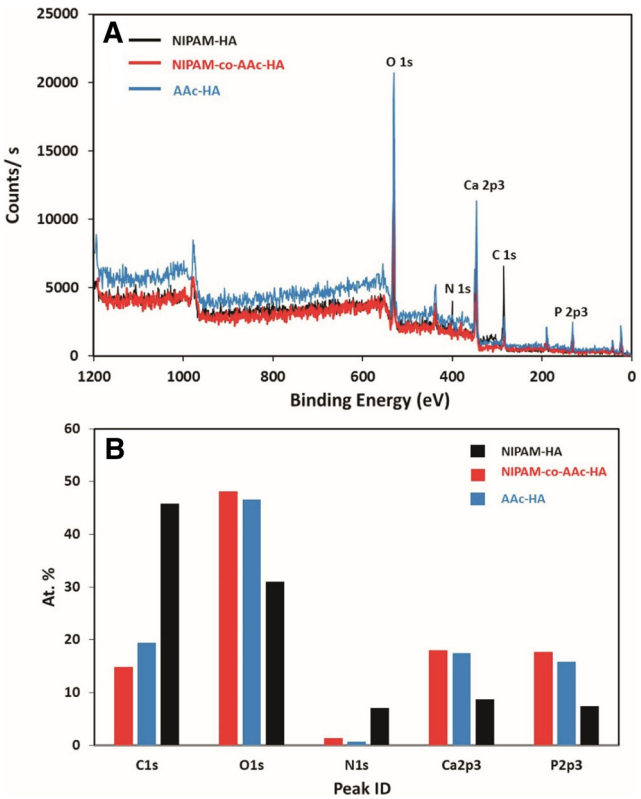

Fig. 9 **a** XPS spectra of NIPAM, NIPAM-co AAc and AAc with HA, (**b**) the atomic percentage of the various peak

The macrostructure and macroscopic phenomenon of the hydrogel on the TPU were obtained by optical microscope (OM). The PNIPAM copolymer with mainly COOH containing co-monomers were already synthesized. In these studies copolymer hydrogel containing chargeable groups were used to increase the adsorption by means of electrostatic interaction. This means that all carboxyl groups of the AAc comonomer are protonated have some surface charges introduced by the initiator during the synthesis. The simultaneous cross-linking of hydrogel and immobilized of hydroxyapatite (HA) showed great influence on the structure and properties, and even the appearance of the UV light-induced graft polymerization hydrogels. The results showed that the NIPAM: AAc (1:1 mol) polymers have large numbers of carboxyl groups and hydroxyl groups result in a favorable adsorption capacity for HA. The SEM micrographs for different regions of bilayered gradient PNIPAM-co-AAc/HA composite hydrogels prepared by different time cycles. As it was expected, the hydrodynamic radius increases with increasing AAc content because of the increasing electrostatic repulsion between the polymer chains and an increase in the osmotic pressure. Alternate soaking process 2 h per cycle were more HA immobilized than 1 h per cycle. We examined HA hybridized PNIPAM-co-AAc stability by comparing digital photos and amount of HA (mg/cm^2) produced by samples stored for different time periods (fresh preparation and 4 months after). The results were shown below, and indicated that amount of HA were observed for 4 months storage. The HA hybridized PNIPAM-co-AAc of remained 92% after 4 months for each groups. The figure was shown in supplementary materials Fig. S1.

FT-IR spectra and XRD pattern of the HA treated different time in the hydrogel networks. The PNIPAM-co-AAc networks, FT-IR spectrum exhibits the characteristic absorption bands of PNIPAM 1664 cm^{-1} for C = O and AAc 3082 cm^{-1} for N-H. Compare with different time per cycle, the HA characteristic peak show at 560, 606 cm^{-1} for P-O and 3600–3100 cm^{-1} presenting a wide characteristic band for water molecules adsorbed on the surface of powder. The peaks of the HA at 25.35°and 31.23°were assigned to reflections on the (002) and (211) planes of the face-centered cubic HA, respectively, confirming that HA existed in the hydrogel. We examined the improvements of the proposed polymerization method in our system. The results will demonstrate that the interplay between intrapolymer and interpolymer aggregation can be tuned by changing factors such as the concentration of AAc, incorporate charged groups onto the AAc chains (−COOH), or adding low temperature plasma processing of HMDSZ/O_2 on TPU. In addition, effect of HA hybridized behavior is analyzed.

HA/hydrogels have been used in many fields, such as tissue engineering, drug delivery and divalent heavy metal ion removal. However, it is still a big challenge to devise an efficient approach for fabricating multi-sensitive smart solid/polymer/liquid interfaces, which is an important step towards the utilization of surface-confined smart polymers as building blocks for biomimetics.

Acknowledgments The authors are grateful for the financial support provided by the Ministry of Science and Technology (MOST) through grant No. MOST 106-2221-E-036-025.

References

1. Clarke J, Vincent B (1981). J Chem Soc Faraday Trans 77:1831
2. Antionietti M, Pakula T, Bremser W (1995). Macromolecules 28: 4227
3. Frank M, Burchard W (1991). Makromol Chem Rapid Commun 12:645
4. Odian G (2004) Principles of polymerization4th edn. Wileye, New York, p 198
5. Yagci Y, Jockusch S, Turro JN (2010). Macromolecules 43:6245
6. Neyrer S, Vincent B (1997). Polymer 38:6129
7. Nodar AM, Zhu KZ, Kjoniksen AL, Kenneth DK, Karlsson G, Bo N (2009). J Phys Chem B 113:11115
8. Stephan S, Hubert M, Thomas H, Regine von K (2008). Polymer 49:749
9. Yang M, Zhao KS (2016). Soft Matter 12:4093
10. Zhao Y, Shi C, Yang XD, Shen B, Sun YQ, Chen Y, Xu XW, Sun HC, Yu K, Yang B, Lin Q (2016). ACS Nano 10:5856
11. Sperling L, Hu R (2014) Polymer Blends Handbook, Springer, pp 677–724
12. Sperling LH, 100+ years of plastics. Leo Baekeland and beyond, Am Chem Soc, 2011, ch 5, 1080, pp. 69–82
13. Lipatov YS, Alekseeva TT, Phase-separated interpenetrating polymer networks, Springer, 2007
14. Chen Y, Chen YB, Nan JY, Wang CP, Chu FX (2012). J Appl Polym Sci 124:4678
15. Chen F, Zhu YJ (2014). Curr Nanosci 10:465
16. Lu BQ, Zhu YJ, Chen F (2014). Chem Eur J 20:1242
17. Zhao XY, Zhu YJ, Chen F, Lu BQ, Wu J (2013). Cryst Eng Comm 15:206
18. Chen F, Zhu YJ, Wang KW, Zhao KL (2011). Cryst Eng Comm 13: 1858
19. Hui JF, Wang X (2011). Chem Eur J 17:6926
20. Zhang YG, Zhu YJ, Chen F, Wu J (2015). Mater Lett 144:35
21. Jiang YY, Zhu YJ, Chen F, Wu J (2015). Ceram Int 41:6098
22. Qi C, Tang QL, Zhu YJ, Zhao XY, Chen F (2012). Mater Lett 85:71
23. Reardon PJT, Handoko AD, Li L, Huang J, Tang JW (2013). J Mater Chem B 1:6170
24. Yang Z, Huang Y, Chen ST, Zhao YQ, Li HL, Hu ZA (2005). J Mater Sci 40:1121
25. Costa DO, Dixon SJ, Rizkalla AS (2012). ACS Appl Mater Interfaces 4:1490
26. Cao MH, Wang YH, Guo CX, Qi YJ, Hu CW (2004). Langmuir 20: 4784
27. Jiang YY, Zhu YJ, Li H, Zhang YG, Shen YQ, Sun TW, Chen F (2017). J Colloid Interface Sci 497:266
28. Anamarija R, Antonia R, Igor GGF, Inga M, Marica I, Hrvoje I (2017). Carbohydr Polym 166:173